PHILOSOPHICAL TRANSACTIONS A

royalsocietypublishing.org/journal/rsta

Review

Cite this article: Horányi M, Szalay JR, Wang X. 2024 The lunar dust environment: concerns for Moon-based astronomy. *Phil. Trans. R. Soc. A* **382**: 20230075.
https://doi.org/10.1098/rsta.2023.0075

Received: 30 June 2023
Accepted: 3 October 2023

One contribution of 13 to a discussion meeting issue 'Astronomy from the Moon: the next decades (part 2)'.

Subject Areas:
space exploration

Keywords:
moon, dust hazard, near-surface dusty plasmas

Author for correspondence:
Mihály Horányi
e-mail: horanyi@colorado.edu

THE ROYAL SOCIETY PUBLISHING

The lunar dust environment: concerns for Moon-based astronomy

Mihály Horányi[1], Jamey R. Szalay[2] and Xu Wang[1]

[1]Laboratory for Atmospheric and Space Physics, and Department of Physics, University of Colorado, Boulder, CO, USA
[2]Department of Astrophysical Sciences, Princeton University, Princeton, NJ, USA

MH, 0000-0002-5920-9226; JRS, 0000-0003-2685-9801; XW, 0000-0001-8472-7079

The Moon has no atmosphere, hence, it offers a unique opportunity to place telescopes on its surface for astronomical observations. It is phase-locked with Earth, and its far side remains free from ground-based interference, enabling the optimal use of radio telescopes. However, the surface of the Moon, as any other airless planetary object in the solar system, is continually bombarded by interplanetary dust particles that cause impact damage and generate secondary ejecta particles that continually overturn the top layer of the lunar regolith. In addition, there is evidence, that small particles comprising the lunar regolith can be electrically charged, mobilized and transported, also representing a hazard for covering sensitive surfaces and interfering with exposed mechanical structures. In addition to the naturally occurring dust transport, rocket firings during landings and take-offs, pedestrian and motorized vehicle traffic will also liberate copious amounts of dust, representing a potential hazard for the safe and optimal use of optical platforms.

This article is part of a discussion meeting issue 'Astronomy from the Moon: the next decades (part 2)'.

1. Introduction

The surface of the Moon is covered with a layer of loose rocky material, including micron and submicron-sized dust particles. This regolith has been formed and remains

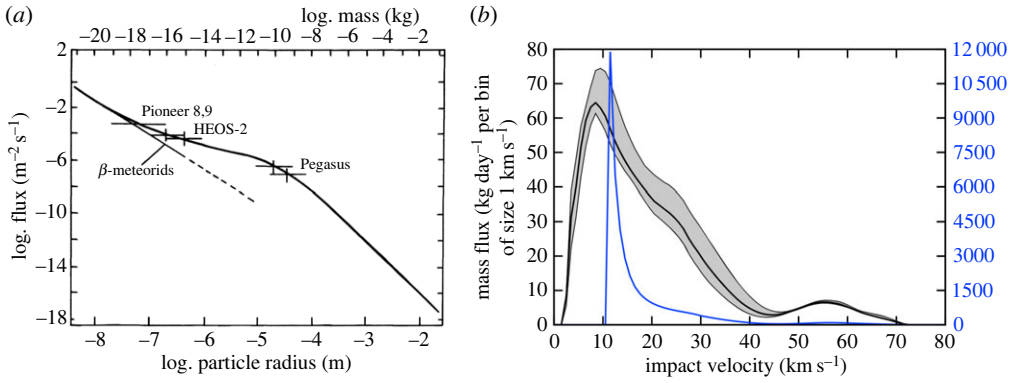

Figure 1. (*a*) The flux of interplanetary meteoroids at 1 AU as a function of their size (mass), the labels indicate space missions, and β-meteoroids are IDPs on escaping orbits driven by radiation pressure [9]; (*b*) the modelled speed distribution, independent of the size of a meteoroid, scaled with the mass flux at the Moon (black solid line) and at Earth (blue solid line) [11,12].

continually reworked, by the intermittent impacts of comets, asteroids, meteoroids and the continual bombardment by interplanetary dust particles (IDPs). All planetary bodies in the inner solar system are continually bombarded by IDPs originating primarily from asteroid collisions and cometary activity. Thick atmospheres protect Venus, Earth and Mars, ablating the incoming IDPs into 'shooting stars' that rarely reach the surface. On the contrary, the surface of airless planetary bodies are directly exposed to IDP impacts. The effects of meteoroids bombarding the lunar surface, especially their contribution to sustaining the tenuous lunar atmosphere, have been recognized since the Apollo era, but there are still large uncertainties in our knowledge about the variability of their flux, size and speed distributions [1]. In addition, the solar wind plasma flow and solar ultraviolet radiation also reach the surface generating a near-surface plasma environment that can lead to charging, mobilization and transport of the lunar fines.

Dust poses risks to human presence or the long-term remote operation of astronomical telescopes on the lunar surface. Dust particles damage spacesuits [2], cover optical surfaces [3–5] and degrade the performances of thermal radiators and solar panels [2]. Lunar dust in human living quarters could lead to health risks when inhaled by astronauts [6].

Below we discuss the effects of the IDP influx (§2), the properties of the secondary ejecta particles they generate (§3) and the near-surface plasma effects on the lunar regolith (§4), as these all represent a potential hazard for establishing permanent human habitats, and to use the unique opportunity the Moon offers to deploy astronomical observatories [7,8]. We offer our assessment for ranking the potential risk these processes represent (§5).

2. Interplanetary dust bombardment

The surfaces of airless bodies near 1 AU are directly exposed to high-speed ($\gg 1\,\mathrm{km\,s^{-1}}$) micrometeoroid impacts, particles with characteristic radii of $\simeq 100\,\mu\mathrm{m}$ dominating the mass flux of $F \simeq 1.5 \times 10^{-15}\,\mathrm{kg\,m^{-2}\,s^{-1}}$ [9]. The most recent estimate of the cosmic dust input into the Earth's atmosphere is (43 ± 14) tons per day [10]. The mass flux of meteoroids impacting the lunar surface is about 30 times smaller due to the Moon's smaller size and reduced gravitational focusing, resulting in an average total deposition rate of (1.4 ± 0.5) tons per day [11]. IDPs arrive at the lunar surface with a characteristic speed of $\simeq 10\,\mathrm{km\,s^{-1}}$ [11]. Figure 1 shows the size, $g(m)$, and speed, $h(v)$, distributions that are assumed to be independent, hence $f(m, v) \simeq g(m) \times h(v)$. The IDP sources impacting the Moon at high latitudes remain largely uncharacterized due to the lack of optical and radar observations in the polar regions on Earth [13]. High-latitude sources

could have very large impact speeds in the range of $30 \leq v \leq 50\,\mathrm{km\,s^{-1}}$ [14,15], hence they are expected to have a significant effect on the lunar surface, including the removal and burial of volatile deposits in the lunar polar regions.

(a) Concern for lunar-based astronomy

IDP impacts will excavate craters on exposed surfaces. One of the goals of NASA's Long Duration Exposure Facility mission (LDEF) was to survey the interplanetary and Earth-orbital dust populations [16]. LDEF was placed in low-Earth orbit (LEO) by the space shuttle Challenger in April 1984, and retrieved by the space shuttle Columbia in January 1990, orbiting for 5.77 years in the altitude range of 331–480 km. After retrieval, a set of 761 craters was identified on a $5.6\,\mathrm{m^2}$ zenith-facing aluminium alloy panel, with diameters in the approximate range of 10 µm–1 mm [17]. Each micrometeoroid impact generates a dent, with a radius and depth set by its mass, speed and composition, degrading the performance of optical surfaces at an approximate rate of 0.01%/year at 1 AU distance from the Sun, with large possible fluctuations due to the stochastic nature of impacts. In the first approximately six months of operations, the Webb telescope's primary mirror, with a total surface area of about $30\,\mathrm{m^2}$, was hit five times, without generating any noticeable degradation in its performance [12]. During the predickted lifetime of 20 years, the Webb telescope's primary mirror is expected to steadily accumulate damages that only minimally degrade its performance, neglecting additional damages by the rare and hard-to-predict larger ($\gg$10 µm) IDPs. Similar degradation is expected for optical telescopes on the lunar surface.

3. High-altitude dust ejecta cloud

In addition to direct damage, IDP impacts generate secondary ejecta particles, lofting them to high altitudes ($\gg$100 km), some even escaping the Moon. The bound ejecta particles form a permanently present dust cloud engulfing the Moon that was identified during NASA's Lunar Atmosphere and Dust Environment Explorer (LADEE) mission [18]. LADEE was launched in September 2013, it reached the Moon in about 30 days, and continued with an instrument checkout period of about 40 days at an altitude range of 220–260 km, followed by approximately 150 days of science observations period at a typical altitude range of 20–100 km. LADEE followed a near-equatorial retrograde orbit, with a characteristic orbital speed of $1.6\,\mathrm{km\,s^{-1}}$. It carried the Lunar Dust Experiment (LDEX) that was designed to explore the ejecta cloud generated by sporadic interplanetary dust impacts, including possible intermittent density enhancements during meteoroid showers, and to search for the putative regions with high densities of dust particles with radii $\ll 1$ µm lofted above the terminators [19]. LDEX was an impact ionization dust detector that measured both the positive and negative charges of the plasma cloud generated when a dust particle struck its target. The amplitude and shape of the waveforms (signal versus time) recorded from each impact were used to estimate the mass of the dust particles. The instrument had a total sensitive area of $0.01\,\mathrm{m^2}$, gradually decreasing to zero for particles arriving from outside its dust field-of-view (FOV) of $\pm 68^\circ$ off from the normal direction [20]. The measured fluxes indicated that the Moon is engulfed in a permanently present, but highly variable dust exosphere (figure 2). The density of the dust exosphere, compared with our best models of the incoming primary meteoroid flux, is lower than expected. Based on LDEX observations, the total ejecta production rate on the Moon is of the order of $18\,\mathrm{t\,day^{-1}}$, indicating a mass yield $Y(\mathrm{mass_{secondary}}/\mathrm{mass_{primary}}) \simeq 10$ [11], 2–3 orders of magnitude smaller than the icy Galilean moons of Jupiter [23].

(a) Concern for lunar-based astronomy

The vast majority of the ejecta particles are launched into a narrow cone angle normal to the surface with speeds below the escape speed from the Moon ($2.4\,\mathrm{km\,s^{-1}}$), hence following ballistic trajectories and returning to the surface [24]. LDEX observations enable us to estimate the average

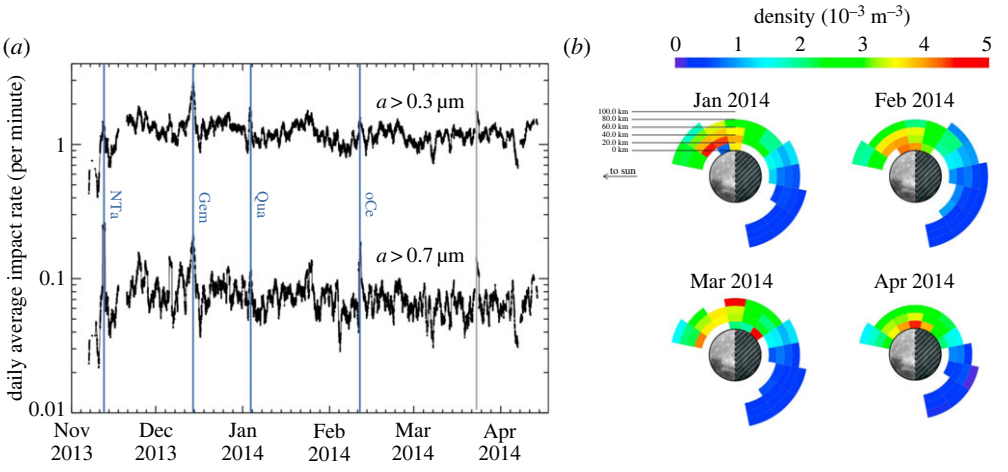

Figure 2. (*a*) The daily running average of impacts per minute of particles with radii $> 0.3\,\mu$m and $a > 0.7\,\mu$m recorded by LDEX. Four annual meteoroid showers generated elevated impact rates lasting several days. The labelled annual meteor showers (blue vertical lines) are the Northern Taurids (NTa); the Geminids (Gem); the Quadrantids (Qua); and the Omicron Centaurids (oCe). Towards the end of March LDEX data indicated a meteor shower that remained unidentified by ground-based observers [19]. (*b*) The average dust ejecta cloud density observed by LDEX for each calendar month LADEE was operational in 2014. Each colour ring corresponds to the density every 20 km. The plot is in a reference frame where the Sun is on the left ($-x$ direction) and the apex motion of the Moon about the Sun is towards the top of the page ($+y$ direction) [21,22]. The missing bottom left quadrants represent data gaps, as LDEX could not make measurements while the Sun was in its FOV.

lunar dust ejecta density distribution above the Moon, and the rate at which this exospheric dust rains back onto the lunar surface. Near the equatorial plane, the burial rate is estimated to be approximately $40\,\mu\mathrm{m\,Myr}^{-1}$ of lunar regolith, with a cumulative size distribution index of $\gamma = 2.7$, $(n(>a) \sim a^{-\gamma})$, that is redistributed due to meteoritic bombardment, a process that occurs predominantly on the lunar apex hemisphere [25]. This burial rate is rather modest; however, it does not include any contribution that initially slow particles, which did not rise to the orbital altitude of LADEE, might contribute.

Additional sources of damage are the fast secondary ejecta particles that have speeds above the lunar escape speed, generated at shallow angles [26]. They dominate the generation of micro craters with diameters below $7\,\mu$m observed on lunar rocks [27,28]. The cratering rate of these small pits, compared with the predictions based on *in situ* measurements of micrometeoroids in space, indicate a flux of fast ejecta $\simeq 10\,\mathrm{m}^{-2}\,\mathrm{s}^{-1}$ of particles with radii $\sim 1\,\mu$m [9], that generates a negligibly slow surface degradation rate due to cratering. However, high-speed hits can generate significant impact charges and electromagnetic pulses and can destroy sensitive electronics [29].

4. Near-surface dust mobilization

Compared with direct IDP impacts (§2), or impacts/burial by secondary ejecta particles (§3), perhaps the biggest concern for Moon-based astronomy is electrostatic dust charging, mobilization and transport, which is expected to dominate the near surface ($\ll 1\,$km) dust environment [30,31]. The Moon has no global magnetic field and only a tenuous exosphere, hence, its surface is directly exposed to the solar wind plasma flow, the Earth's magnetospheric plasma environment and solar ultraviolet (UV) radiation, resulting in electric charging of the regolith that varies in space and time [32]. Electrostatic charges are expected to accumulate on human and robotic exploration systems, causing potential issues for crew safety and for the performance of scientific instruments and equipment [33–36].

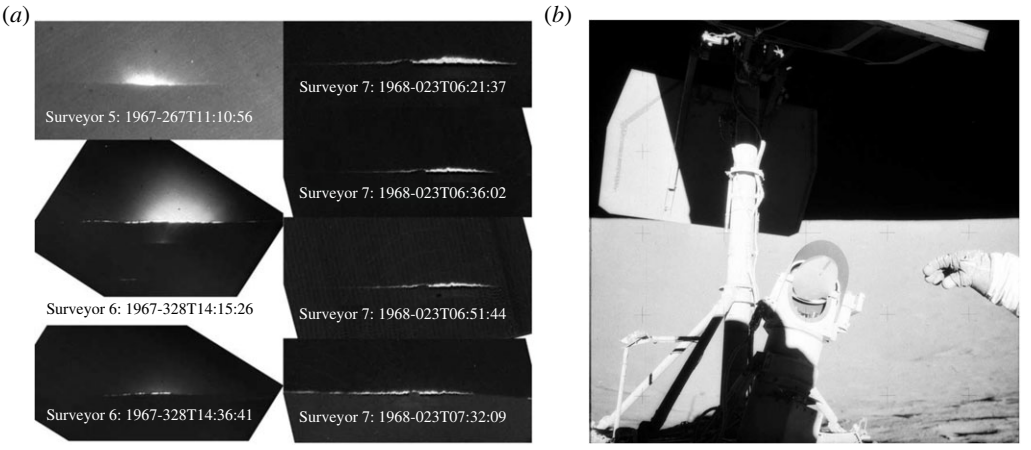

Figure 3. (*a*) Images of lunar horizon glow. The contribution of Zodiacal light is evident in Surveyor 5 and 6 but not in Surveyor 7 images, perhaps because of the different camera iris settings. (*b*) Apollo 12 Charles 'Pete' Conrad Jr. gestures near the Surveyor 3 spacecraft on the lunar surface on 21 November 1969. The Surveyor 3 television mirror shows a finger mark made by Conrad in a layer of dust on the mirror. Surveyor 3 landed on the Moon on 20 April 1967. Dust was likely deposited on the mirror both during the landing of the Surveyor and also during the landing of the Apollo 12 Lunar Module 155 m away (photos are from NASA's Science Data Center).

Electrostatic processes on the lunar surface were first indicated by Apollo-era observations. The Lunar Horizon Glow (LHG), 30 cm above the surface was recorded shortly after sunset by the Surveyor landers (figure 3). The LHG is likely due to sunlight scattered off a cloud of dust particles with radii of a few µm that are lofted by electrostatic forces near the terminator [37–40]. The height of the LHG is consistent with a recent observation by the Chang'E-3 rover of fine dust deposits on lunar rocks up to a height of $\simeq$30 cm [41].

The unexpected signals of the Apollo 17 Lunar Ejecta and Meteorites Experiment (LEAM) deployed on the lunar surface have been suggested to be due to low-speed ($<100\,\mathrm{m\,s^{-1}}$), highly charged dust particles with the rates spiking near sunset and sunrise [42]. However, different LEAM datasets showed no rate enhancement associated with terminator crossings and indicated that any enhancements were likely caused by rapid temperature changes rather than lofted dust [43]. Similarly, high-altitude dust possibly lofted through electrostatic mechanisms indicated from the Apollo astronauts' sketches [44,45] and images from orbit [46,47] remained controversial. Such a dust population was not confirmed by the remote sensing observations by Clementine [48] and LRO/LAMP [49], or by the *in situ* measurements from LADEE/LDEX [21,50], contrary to a competing analysis [51]. These putative near-surface dust mobilizations might represent only modest dust fluxes, as opposed to dust mobilization due to human activities (figure 3), but they are acting continually for long periods of time, and without easy mission design solutions to mitigate their effects.

Through the decades following the Apollo missions, the processes responsible for the initial lift-off of dust particles remained poorly understood, even though a number of models [52–54] and laboratory experiments [55–58] were dedicated to this issue and succeeded in explaining the subsequent dynamics of charged dust particles in plasma sheaths. Recently, the recognition of the roles micro-cavities play in surface charging led to a better understanding of particle lift-off from surfaces due to plasma effects, the so-called patched charge model [59]. The model, verified by a series of experiments (figure 4) [60–66], is based on the emission and re-absorption of secondary electrons, generated by impacting energetic ($\gg$1 eV) electrons, ions or UV photons. As opposed to the case of a flat surface, secondary electrons can remain trapped in cavities that form between dust particles, generating a potential difference of the order of 2–3 V, due to the typical energy of secondary electrons. This potential difference for a photoelectron plasma sheath

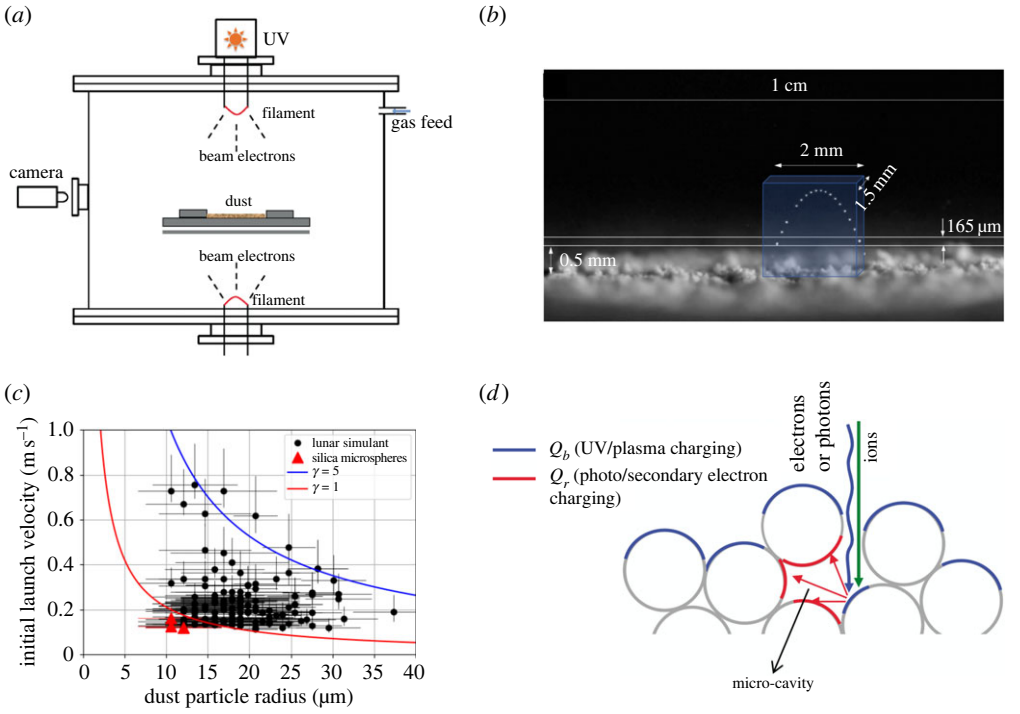

Figure 4. (*a*) The schematic of the experimental set-up to investigate dust charging, mobilization and transport under UV and/or plasma exposure of a regolith surface [59–62]. (*b*) Stacked images of the trajectory of a single dust particle lofted from the surface, using a narrow focal plane normal to the boresight of the camera. Images like this are used to measure the initial speed of the particle [62]. (*c*) Initial launch velocities as a function of dust size for irregularly shaped lunar simulant particles (circles) and 10 µm radius silica microspheres (triangles). The theoretical curves (solid lines), obtained from energy conservation, are shown with $\gamma = 1$ and 5 that parameterize the cohesion between particles [62]. (*d*) Cartoon of the 'patched charge model' [59].

on the Moon, with a daytime characteristic shielding thickness of the order of 1 m, generates an electric field ≃2 to 3 V m^{-1}. In a cavity, the same potential difference develops across characteristic distances of perhaps 10 to 100 µm, generating surprisingly large electric fields of the order of 10–100 kV m^{-1}, accompanied by highly enhanced, both positive and negative surface charge density distributions. The combination of complex electric fields and charge density distributions leads to 'Coulomb explosions', which break the cohesive forces between dust particles, and lead to the initial lift-off of charged grains (figure 4) [59]. Contrary to the expectations of positively charged particles, the emergence of highly negatively charged particles from a rough surface under UV illumination has been verified in laboratory experiments [60] and successfully explained using computer simulations [67].

(a) Concern for lunar-based astronomy

The lunar soil samples, returned by the Apollo missions, have a size range of 1 µm to 1 cm and an approximately log-normal size distribution with a typical maximum in the range of 60–120 µm [68,69]. The small optical dust detectors on Apollo 12, 14 and 15 [70], each placed 1 m above the surface, indicated a combined long-term dust accumulation rate of the order of 100 µg cm^{-2} y^{-1} [71]. The Chang'E-3 lander's Sticky Quartz Crystal Microbalance (SQCM), at a height of 1.9 m above the lunar surface, reported a dust accumulation rate of about 20 µg cm^{-2} y^{-1} [72]. Without knowing the initial speed and velocity distribution of the dust grains launched from the surface, it

remains an open question how the dust accumulation rate changes with height above the surface. Assuming that these were similar at all the Apollo and the ChangE'3 landing sites, and using the observations at these two distinct heights to determine an approximate scale height, assuming that $\dot{m} = \dot{m}_0 \exp(-h/h_0)$ for dust deposition, indicates $h_0 \simeq 0.6$ m, and an accumulation rate $\dot{m}_0 = 500\,\mu g\,cm^{-2}\,y^{-1}$ on the surface. If the characteristic radius of the mobilized dust particles is $a = 10\,\mu m$, the coverage of an exposed flat surface ($h = 0$) by dust is about 15%/y, if a $= 50\,\mu m$ the coverage is 3%/y, and if $a = 100\,\mu m$, the coverage reduces to 1.5%/y.

The size and initial speed distributions of lofted particles were measured in laboratory experiments (figure 4), establishing an expected lofting rate, if extrapolated to lunar conditions, of 1–10 $cm^{-2}\,s^{-1}$ [61]. While in the tabletop laboratory experiments this initial rate dropped in minutes due to a lack of reciprocal dust transport in/out of the small crater holding the lunar simulant, it is expected that the dust lofting rates on the lunar surface could be sustained over geological timescales. The typical lift-off speed of $\simeq 0.5\,m\,s^{-1}$ in these experiments indicates that the particles in the typical size of 10 to 20 μm could reach heights of > 10 cm on the lunar surface. If 10 μm particles are lofted at a rate of 1 $cm^{-2}\,s^{-1}$ they generate a surface coverage rate of nearly 30% per day of landing particles. Some of the deposited grains could be subsequently removed by the very same processes, but dust mobilization from a smooth surface covered by a single layer of dust is expected to be much less efficient. The laboratory experiments cannot possibly reproduce lunar vacuum, UV radiation and plasma conditions, or the properties of the regolith, hence, the efficacy of plasma and UV-induced dust charging, mobilization and transport on the lunar surface remains an open issue. It is perhaps still encouraging that the rough estimates based on the combined Apollo [71] and ChangE'3 [72] *in situ* measurements are of similar magnitude as the laboratory results [61]. These processes could represent a significantly large enough hazard to warrant a combination of *in situ* measurements.

5. Conclusion

Dust on the lunar surface represents a variety of hazards and its safe and effective mitigation requires detailed, yet to-be-fully developed, engineering approaches. The lunar dust is extremely abrasive, similar to broken glass, it ruins friction-bearing surfaces, seals, gaskets, optical lenses, windows, degrades thermal radiators, solar panels and causes dangerous physiological effects on the tissue in human lungs [2].

Solar panels and optical devices on the lunar surface will lose performance due to the accumulation of dust particles on their surfaces. However, it is possible that dust accumulation can reach equilibrium due to the accompanying processes that can lead to concurrent dust removal. The Apollo Lunar Laser Retroreflectors deployed during Apollo 11, 14 and 15 are still operating after well over 40 years; however, the magnitude of the return signal has decreased by a factor of 10 to 100 since the arrays were deployed [3–5]. Even at the very start of their use, the strength of the return signal was about 10% of the expected value, based upon an analysis of the ground stations and the retroreflector arrays. A deposit of lunar dust on the front faces of the reflectors is the most likely reason, other causes have also been suggested, for example, the darkening of the glass material due to UV and/or particle exposure, micrometeoroid bombardment, or change in the thermal properties due to dust, UV and or plasma exposure. The dust may be due to secondary ejecta from micrometeorite impacts in the vicinity, electrically levitated dust and/or dust from the lift-off of the Apollo lunar module [4].

Most open questions about near-surface dust mobilization could be answered by precursor missions delivering small dedicated experiments to the lunar surface. For example, the size and speed distributions of electrostatically levitated dust could be measured on the surface [73,74]. A complementary measurement of the dust coverage as a function of height could be measured by the optical transmission changes of a series of glass plates [75] or quartz crystal microbalance set-ups [72].

We focused on the naturally occurring dust hazards, but rocket firings during landings and take-offs, pedestrian and motorized vehicle traffic, for example, will liberate copious amounts

of dust, representing a potential hazard for the safe and optimal use of optical platforms [76]. These, however, could be mitigated by careful mission design using distant landing/take-off sites, minimizing any traffic near installations and by including shutters and covers over sensitive surfaces that can be deployed during critical periods, as needed. Site selections for the various scientific installations, and their long-term optimal use, will require international agreements and cooperations [77].

Data accessibility. This article has no additional data.

Declaration of AI use. We have not used AI-assisted technologies in creating this article.

Authors' contributions. M.H.: formal analysis, funding acquisition, investigation, writing—original draft; X.W.: investigation, methodology, writing—review and editing; J.R.S.: investigation, methodology, software, visualization, writing—review and editing.

All authors gave final approval for publication and agreed to be held accountable for the work performed therein.

Conflict of interest declaration. We declare we have no competing interests.

Funding. The authors acknowledge support from NASA's Solar System Exploration Reserach Virtual Institute (SSERVI): Institute for Modeling Plasmas, Atmopsheres, and Cosmic Dust (IMPACT).

References

1. Janches D, Berezhnoy AA, Christou AA, Cremonese G, Hirai T, Horányi M, Jasinski JM, Sarantos M. 2021 Meteoroids as one of the sources for exosphere formation on airless bodies in the inner solar system. *Space Sci. Rev.* **217**, 50. (doi:10.1007/s11214-021-00827-6)
2. Taylor LA, Schmitt HH, Carrier III WD, Nakagawa M. 2005 The lunar dust problem: from liability to asset. In *AIAA 1st Space Exploration Conf.: Continuing the Voyage of Discovery*, vol. 1, pp. 1–8.
3. Murphy Jr TW, Adelberger EG, Battat JBR, Hoyle CD, McMillan RJ, Michelsen EL, Samad RL, Stubbs CW, Swanson HE. 2010 Long-term degradation of optical devices on the Moon. *Icarus* **208**, 31–35. (doi:10.1016/j.icarus.2010.02.015)
4. Currie DG, Delle Monache G, Dell'Agnello S, Murphy T. 2013 Dust degradation of apollo lunar laser retroreflectors and the implications for the next generation lunar laser retroreflectors. In *AGU fall meeting abstracts*, vol. 2013, pp. P51G–1815.
5. Murphy Jr TW, McMillan RJ, Johnson NH, Goodrow SD. 2014 Lunar eclipse observations reveal anomalous thermal performance of Apollo reflectors. *Icarus* **231**, 183–192. (doi:10.1016/j.icarus.2013.12.006)
6. Lam CW *et al.* 2008 Pulmonary Toxicity Studies of Lunar Dust in Rodents. In *NLSI Lunar Science Conference*, vol. 1415, LPI Contributions, p. 2136.
7. Silk J, Crawford I, Elvis M, Zarnecki J. 2021 Astronomy from the Moon: the next decades. *Phil. Trans. R. Soc. A* **379**, 20190560. (doi:10.1098/rsta.2019.0560)
8. Silk J, Crawford I, Elvis M, Zarnecki J. 2023 The next decades for astronomy from the Moon. *Nat. Astron.* **7**, 648–650. (doi:10.1038/s41550-023-02000-1)
9. Grun E, Zook HA, Fechtig H, Giese RH. 1985 Collisional balance of the meteoritic complex. *Icarus* **62**, 244–272. (doi:10.1016/0019-1035(85)90121-6)
10. Carrillo-Sánchez JD, Nesvorný D, Pokorný P, Janches D, Plane JMC. 2016 Sources of cosmic dust in the Earth's atmosphere. *Geophys. Res. Lett.* **43**, 11. (doi:10.1002/2016GL071697)
11. Pokorný P, Janches D, Sarantos M, Szalay JR, Horányi M, Nesvorný D, Kuchner MJ. 2019 Meteoroids at the Moon: orbital properties, surface vaporization, and impact ejecta production. *J. Geophys. Res.* (*Planets*) **124**, 752–778. (doi:10.1029/2018JE005912)
12. Witze A. 2022 Surprising dust strike on Webb telescope has scientists on alert. *Nature* (doi:10.1038/d41586-022-01877-8)
13. Pokorný P, Sarantos M, Janches D, Mazarico E. 2020 Meteoroid bombardment of lunar poles. *Astrophys. J.* **894**, 114. (doi:10.3847/1538-4357/ab83ee)
14. Campbell-Brown M, Wiegert P. 2009 Seasonal variations in the north toroidal sporadic meteor source. *Meteorit. Planet. Sci.* **44**, 1837–1848. (doi:10.1111/j.1945-5100.2009.tb01992.x)
15. Pokorný P, Vokrouhlický D, Nesvorný D, Campbell-Brown M, Brown P. 2014 Dynamical model for the toroidal sporadic meteors. *Astrophys. J.* **789**, 25. (doi:10.1088/0004-637X/789/1/25)

16. McDonnell JAM. 1992 Impact cratering from LDEF's 5.75-year exposure: decoding of the interplanetary and earth-orbital populations. In *Lunar and Planetary Science Conf. Proc.*, vol. 22, pp. 185–193.
17. Love SG, Brownlee DE. 1993 A direct measurement of the terrestrial mass accretion rate of cosmic dust. *Science* **262**, 550–553. (doi:10.1126/science.262.5133.550)
18. Elphic RC, Delory GT, Hine BP, Mahaffy P, Horanyi M, Colaprete A, Benna M, Noble S. 2014 The lunar atmosphere and dust environment explorer mission. *Space Sci. Rev.* **185**, 3–25. (doi:10.1007/s11214-014-0113-z)
19. Horányi M, Szalay JR, Kempf S, Schmidt J, Grün E, Srama R, Sternovsky Z. 2015 A permanent, asymmetric dust cloud around the Moon. *Nature* **522**, 324–326. (doi:10.1038/nature14479)
20. Horányi M *et al.* 2014 The lunar dust experiment (LDEX) onboard the lunar atmosphere and dust environment explorer (LADEE) mission. *Space Sci. Rev.* **185**, 93–113. (doi:10.1007/978-3-319-18717-45)
21. Szalay JR, Horányi M. 2015 The search for electrostatically lofted grains above the Moon with the Lunar Dust Experiment. *Geophys. Res. Lett.* **42**, 5141–5146. (doi:10.1002/2015GL064324)
22. Szalay JR, Horányi M. 2016 Detecting meteoroid streams with an in-situ dust detector above an airless body. *Icarus* **275**, 221–231. (doi:10.1016/j.icarus.2016.04.024)
23. Krüger H, Krivov AV, Sremčević M, Grün E. 2003 Impact-generated dust clouds surrounding the Galilean moons. *Icarus* **164**, 170–187. (doi:10.1016/S0019-1035(03)00127-1)
24. Bernardoni EA, Szalay JR, Horanyi M. 2019 Impact ejecta plumes at the Moon. *Geophys. Res. Lett.* **46**, 534–543. (doi:10.1029/2018GL079994)
25. Szalay JR, Horányi M. 2016 Lunar meteoritic gardening rate derived from *in situ* LADEE/LDEX measurements. *Geophys. Res. Lett.* **43**, 4893–4898. (doi:10.1002/2016GL069148)
26. Schneider E. 1975 Impact ejecta exceeding lunar escape velocity. *Moon* **13**, 173–184. (doi:10.1007/BF00567514)
27. Zook HA, Lange G, Grun E, Fechtig H. 1984 Lunar primary and secondary microcraters and the micrometeoroid flux. In *Lunar and Planetary Science Conf.*, pp. 965–966.
28. Zook HA, Lange G, Gruen E, Fechtig H. 1985 The interplanetary micrometeoroid flux and lunar primary and secondary microcraters (ir). In *IAU colloq. 85: properties and interactions of interplanetary dust* (eds RH Giese, P Lamy), p. 89.
29. Close S, Colestock P, Cox L, Kelley M, Lee N. 2010 Electromagnetic pulses generated by meteoroid impacts on spacecraft. *J. Geophys. Res.* (*Space Physics*) **115**, A12328. (doi:10.1029/2010JA015921)
30. Grün E, Horányi M, Sternovsky Z. 2011 The lunar dust environment. *Planet. Space Sci.* **59**, 1672–1680. (doi:10.1016/j.pss.2011.04.005)
31. Horanyi M *et al.* 2020 The lunar dust environment. In *The impact of lunar dust on human exploration*, vol. 2141, LPI Contributions, p. 5032.
32. Halekas JS, Saito Y, Delory GT, Farrell WM. 2011 New views of the lunar plasma environment. *Planet. Space Sci.* **59**, 1681–1694. (doi:10.1016/j.pss.2010.08.011)
33. Farrell WM, Stubbs TJ, Delory GT, Vondrak RR, Collier MR, Halekas JS, Lin RP. 2008 Concerning the dissipation of electrically charged objects in the shadowed lunar polar regions. *Geophys. Res. Lett.* **35**, L19104. (doi:10.1029/2008GL034785)
34. Jackson TL, Farrell WM, Zimmerman MI. 2015 Rover wheel charging on the lunar surface. *Adv. Space Res.* **55**, 1710–1720. (doi:10.1016/j.asr.2014.12.027)
35. O'Brien BJ. 2018 Paradigm shifts about dust on the Moon: from Apollo 11 to Chang'e-4. *Planet. Space Sci.* **156**, 47–56. (doi:10.1016/j.pss.2018.02.006)
36. Yeo LH, Wang X, Dove A, Horányi M, 2023 Laboratory investigations of triboelectric charging of dust by rover wheels. *Adv. Space Res.* **72**, 1861–1869. (doi:10.1016/j.asr.2023.05.002)
37. Criswell DR. 1973 Horizon-glow and the motion of lunar dust. In *Photon and particle interactions with surfaces in space*, vol. 37 (ed. RJL Grard), Astrophysics and Space Science Library, p. 545.
38. Rennilson JJ, Criswell DR. 1974 Surveyor observations of lunar horizon-glow. *Moon* **10**, 121–142. (doi:10.1007/BF00655715)
39. Severnyi AB, Terez EI, Zvereva AM. 1975 The measurements of sky brightness on lunokhod-2. *Moon* **14**, 123–128. (doi:10.1007/BF00562978)
40. Colwell JE, Horányi M, Robertson S, Wang X, Haugsjaa A, Wheeler P. 2007 Behavior of charged dust in plasma and photoelectron sheaths. *Dust Planet. Syst.* **643**, 171–175.

41. Yan Q, Zhang X, Xie L, Guo D, Li Y, Xu Y, Xiao Z, Di K, Xiao L. 2019 Weak dust activity near a geologically young surface revealed by Chang'E-3 mission. *Geophys. Res. Lett.* **46**, 9405–9413. (doi:10.1029/2019GL083611)
42. Berg OE, Wolf H, Rhee J. 1976 Lunar soil movement registered by the apollo 17 cosmic dust experiment. In *Interplanetary dust and zodiacal light* (eds H Elsaesser, H Fechtig), vol. 48, p. 233.
43. Grün E, Srama R, Horányi M. 2013 Comparative analysis of the ESA and NASA interplanetary meteoroid environment models. In *6th European Conf. on Space Debris Abstracts*.
44. McCoy JE, Criswell DR. 1974 Evidence for a high altitude distribution of lunar dust. In *Lunar and Planetary Science Conference Proc.*, pp. 2991–3005.
45. Zook HA, McCoy JE. 1991 Large scale lunar horizon glow and a high altitude lunar dust exosphere. *Geophys. Res. Lett.* **18**, 2117–2120. (doi:10.1029/91GL02235)
46. McCoy JE. 1976 Photometric studies of light scattering above the lunar terminator from Apollo solar corona photography. In *Lunar and Planetary Science Conf. Proc.*, pp. 1087–1112.
47. Glenar DA, Stubbs TJ, McCoy JE, Vondrak RR. 2011 A reanalysis of the Apollo light scattering observations, and implications for lunar exospheric dust. *Planet. Space Sci.* **59**, 1695–1707. (doi:10.1016/j.pss.2010.12.003)
48. Glenar DA, Stubbs TJ, Hahn M, Wang Y. 2014 Search for a high altitude lunar dust exosphere using clementine navigational star tracker measurements. *J. Geophys. Res.* **119**, 2548–2567. (doi:10.1002/2014JE004702)
49. Feldman PD *et al.* 2014 Upper limits for a lunar dust exosphere from far-ultraviolet spectroscopy by LRO/LAMP. *Icarus* **233**, 106–113. (doi:10.1016/j.icarus.2014.01.039)
50. Bernardoni E, Horányi M, Szalay JR. 2023 Analyzing LDEX's current measurements in lunar orbit. *Planet. Sci. J.* **4**, 20. (doi:10.3847/PSJ/aca898)
51. Xie L, Zhang X, Li L, Zhou B, Zhang Y, Yan Q, Feng Y, Guo D, Yu S. 2020 Lunar dust fountain observed near twilight craters. *Geophys. Res. Lett.* **47**, e89593. (doi:10.1029/2020GL089593)
52. Nitter T, Havnes O. 1992 Dynamics of dust in a plasma sheath and injection of dust into the plasma sheath above moon and asteroidal surfaces. *Earth Moon Planets* **56**, 7–34. (doi:10.1007/BF00054597)
53. Poppe A, James D, Jacobsmeyer B, Horányi M. 2010 First results from the Venetia Burney Student Dust Counter on the New Horizons mission. *Geophys. Res. Lett.* **37**, 11101. (doi:10.1029/2010GL043300)
54. Poppe AR, Halekas JS, Delory GT, Farrell WM, Angelopoulos V, McFadden JP, Bonnell JW, Ergun RE. 2012 A comparison of ARTEMIS observations and particle-in-cell modeling of the lunar photoelectron sheath in the terrestrial magnetotail. *Geophys. Res. Lett.* **39**, 1102. (doi:10.1029/2011GL050321)
55. Sickafoose AA, Colwell JE, HoráNyi M, Robertson S. 2002 Experimental levitation of dust grains in a plasma sheath. *J. Geophys. Res.* (*Space Physics*) **107**, 1408. (doi:10.1029/2002JA009347)
56. Flanagan TM, Goree J. 2006 Dust release from surfaces exposed to plasma. *Phys. Plasmas* **13**, 123504. (doi:10.1063/1.2401155)
57. Wang X, Horányi M, Robertson S. 2009 Experiments on dust transport in plasma to investigate the origin of the lunar horizon glow. *J. Geophys. Res.* (*Space Physics*) **114**, 5103. (doi:10.1029/2008JA013983)
58. Wang X, Horányi M, Robertson S. 2010 Investigation of dust transport on the lunar surface in a laboratory plasma with an electron beam. *J. Geophys. Res.* (*Space Physics*) **115**, 11102. (doi:10.1029/2010JA015465)
59. Wang X, Schwan J, Hsu HW, Grün E, Horányi M. 2016 Dust charging and transport on airless planetary bodies. *Geophys. Res. Lett.* **43**, 6103–6110. (doi:10.1002/2016GL069491)
60. Schwan J, Wang X, Hsu HW, Grün E, Horányi M. 2017 The charge state of electrostatically transported dust on regolith surfaces. *Geophys. Res. Lett.* **44**, 3059–3065. (doi:10.1002/2017GL072909)
61. Hood N, Carroll A, Mike R, Wang X, Schwan J, Hsu HW, Horányi M. 2018 Laboratory investigation of rate of electrostatic dust lofting over time on airless planetary bodies. *Geophys. Res. Lett.* **45**, 13 206–13 212. (doi:10.1029/2018GL080527)
62. Carroll A, Hood N, Mike R, Wang X, Hsu HW, Horányi M. 2020 Laboratory measurements of initial launch velocities of electrostatically lofted dust on airless planetary bodies. *Icarus* **352**, 113972. (doi:10.1016/j.icarus.2020.113972)

63. Orger NC, Cordova Alarcon JR, Toyoda K, Cho M. 2018 Lunar dust lofting due to surface electric field and charging within micro-cavities between dust grains above the terminator region. *Adv. Space Res.* **62**, 896–911. (doi:10.1016/j.asr.2018.05.027)
64. Orger NC, Toyoda K, Masui H, Cho M. 2019 Experimental investigation on silica dust lofting due to charging within micro-cavities and surface electric field in the vacuum chamber. *Adv. Space Res.* **63**, 3270–3288. (doi:10.1016/j.asr.2019.01.045)
65. Orger NC, Toyoda K, Masui H, Cho M. 2021 Experimental investigation on particle size and launch angle distribution of lofted dust particles by electrostatic forces. *Adv. Space Res.* **68**, 1568–1581. (doi:10.1016/j.asr.2021.03.037)
66. Hood N, Carroll A, Wang X, Horányi M. 2022 Laboratory measurements of size distribution of electrostatically lofted dust. *Icarus* **371**, 114684. (doi:10.1016/j.icarus.2021.114684)
67. Zimmerman MI, Farrell WM, Hartzell CM, Wang X, Horanyi M, Hurley DM, Hibbitts K. 2016 Grain-scale supercharging and breakdown on airless regoliths. *J. Geophys. Res. (Planets)* **121**, 2150–2165. (doi:10.1002/2016JE005049)
68. McKay DS, Fruland RM, Heiken GH. 1974 Grain size and the evolution of lunar soils. In *Lunar and Planetary Science Conf. Proc.*, vol. 1, pp. 887–906.
69. Heiken GH, Vaniman DT, French BM. 1991 *Lunar sourcebook, a user's guide to the moon*. Cambridge, UK: Cambridge University Press.
70. O'Brien L, Grün E, Sternovsky Z. 2015 Optimization of the Nano-Dust Analyzer (NDA) for operation under solar UV illumination. *Planet. Space Sci.* **119**, 173–180. (doi:10.1016/j.pss.2015.09.014)
71. Hollick M, O'Brien BJ. 2013 Lunar weather measurements at three Apollo sites 1969–1976. *Space Weather* **11**, 651–660. (doi:10.1002/2013SW000978)
72. Li D *et al.* 2019 In situ measurements of lunar dust at the Chang'E-3 landing site in the northern Mare Imbrium. *J. Geophys. Res. (Planets)* **124**, 2168–2177. (doi:10.1029/2019JE006054)
73. Wang X, Sternovsky Z, Horanyi M, Deca J, Garrick-Bethell I, Farrell WM, Minafra J, Bucciantini L. 2020 Electrostatic dust analyzer (EDA) for characterizing dust transport on the lunar surface. In *AGU Fall Meeting Abstracts*, vol. 2020, pp. P062-03.
74. Wang X, Sternovsky Z, Horanyi M, Deca J, Garrick-Bethell I, Farrell WM, Minafra J, Bucciantini L. 2021 Electrostatic dust analyzer (EDA) for measuring dust transport on the lunar surface. In *2021 Annual Meeting of the Lunar Exploration Analysis Group*, vol. 2635, LPI Contributions, p. 5019.
75. Doner A, Horányi M, Faller J, Fontanese J, Munsat T. 2021 Restoring light transmission of dusty glass surfaces on the Moon. *Adv. Space Res.* **68**, 4050–4055. (doi:10.1016/j.asr.2021.07.020)
76. Qiao L *et al.* 2023 Extensive lunar surface disturbance at the Chang'e-5 mission landing site: implications for future lunar base design and construction. *J. Geophys. Res.: Planets* **128**, e2022JE007730. (doi:10.1029/2022JE007730)
77. Krolikowski A. 2023 Time to protect scientific opportunity on the Moon. *Nat. Astron.* **7**, 637–639. (doi:10.1038/s41550-023-02002-z)